# Relative importance of trenchward upper plate motion and friction along the plate interface for the topographic evolution of subduction-related mountain belts

ANDREA HAMPEL & ADRIAN PFIFFNER
*Institute of Geological Sciences, University of Bern, Baltzerstr 1, 3012 Bern, Switzerland (e-mail: andrea@geo.unibe.ch)*

**Abstract:** We present finite-element models that investigate the relative importance of both trenchward motion of the upper plate and interplate coupling for the development of topography at convergent margins. Commonly, the role of a trenchward moving continental plate for the growth of topography is neglected in both modelling and field studies. Instead, forces exerted by the downgoing plate on the continental plate as well as interplate coupling are thought to be responsible for the deformation of the upper plate. Our model set-up includes an oceanic plate, which is in contact with a continental plate along a frictional plate interface and driven by slab pull. Both lithospheres have an elasto-visco-plastic rheology. The models demonstrate that friction along the plate interface can only lead to a high topography if the upper plate is moving toward the trench. Without such a trenchward advance, no high topography is generated, as the upper plate subsides owing to the drag exerted by the subducting plate. Increasing the coefficient of friction only amplifies the drag and increases the amount of subsidence. Our findings imply that trenchward motion of the continental plate plays a key role for the development of mountain belts at convergent margins; subduction of an oceanic plate even with high interplate coupling cannot explain the formation of Andean-type orogens.

The growth of topography at convergent margins like the Andean subduction zone has commonly been explained from a point of view that centres on the nature and behaviour of the subducting oceanic plate (Jordan *et al*. 1983; Bott *et al*. 1989; Dewey & Lamb 1992; Shemenda 1993; Willett *et al.* 1993; Gephart 1994; Huang *et al.* 1998; Stern 2002; Lamb & Davis 2003; Nicol & Beavan 2003). In particular, the age and buoyancy of the oceanic plate, its angle of subduction or the ratio between the velocity of plate convergence and of subduction have been drawn upon to explain different styles of deformation in the upper plate (e.g., Molnar & Atwater 1978; England & Wortel 1980; Royden 1993). Furthermore, the material flow in the wedge of mantle between the slab and the overriding plate as well as the viscosity of the mantle wedge have been inferred to modify the topography of the upper plate (Wdowinski *et al.* 1989; Billen & Gurnis 2001). This view assigns a passive role to the overriding plate, which is assumed to react to the forces exerted by the oceanic plate, and neglects the motion of the continental plate.

The use of a framework with an oceanic plate actively moving away from a spreading ridge and sliding down a fixed subduction slot beneath a continent has been criticized by Hamilton (1995, 2003), who emphasizes that oceanic plates subduct because their slabs sink into the mantle owing to their higher density. Hence, the slab pull force acts only in the vertical direction and generally leads to rollback of the slab (e.g., Forsyth & Uyeda 1975; Hamilton 2003). As a consequence, subduction zones (like other plate boundaries) are not stationary and, moreover, downgoing oceanic plates cannot compress their associated upper plates and induce intraplate shortening (Hamilton 1995, 2003). In Jarrard's (1986) comprehensive statistical analysis of the relations between subduction parameters, this is manifested in a poor correlation between the upper plate's strain regime, and the age and other characteristics of the downgoing plate. In contrast, a high correlation exists between the upper plate's strain regime and its absolute motion, which suggests that among the independent subduction parameters the motion of the upper plate is a first-order parameter to control the deformation of the upper plate (Jarrard 1986; Heuret & Lallemand 2005). Likewise, other studies inferred a close relation between the absolute motion

*From*: BUITER, S. J. H. & SCHREURS, G. (eds) 2006. *Analogue and Numerical Modelling of Crustal-Scale Processes.* Geological Society, London, Special Publications, **253**, 105–115.
0305-8719/06/$15.00 

of the overriding plate and backarc extension or shortening (Chase 1978; Uyeda & Kanamori 1979; Ruff & Kanamori 1980; Scholz & Campos 1995; Conrad *et al.* 2004).

Another first-order factor discussed as relevant for mountain building in the upper plate is the degree of interplate coupling (e.g., Dmowska *et al.* 1996; Cattin *et al.* 1997; Wang & He 1999; Bevis *et al.* 2001; Husson & Ricard 2004; Yanez & Cembrano 2004). In fact, the topographic profile of the upper plate has been used to *infer* high coefficients of friction and shear stresses along a plate interface, for example for the Andes (Lamb & Davis 2003) or northeast Japan (Huang *et al.* 1997). While Lamb & Davis (2003) and Huang *et al.* (1997) ultimately link the high interplate coupling to the subduction of the oceanic plate, other studies point out the close correlation between high seismic coupling and the trenchward advance of the upper plate (Uyeda & Kanamori 1979; Ruff & Kanamori 1980; Conrad *et al.* 2004). Numerical modelling studies on the influence of friction on topography also reached different conclusions about the role of friction in a subduction system (Cattin *et al.* 1997; Hassani *et al.* 1997; Buiter *et al*. 2001). Hassani *et al.* (1997) constructed finite-element models and assigned an effective elastic thickness to the lower and upper plate. Their upper plate was fixed, while a horizontal velocity and a slab pull force were imposed on the ridgeward and trenchward ends of the oceanic plate, respectively. The models were calculated with friction coefficients of $\mu = 0$, 0.1, 0.2 and 0.5. For all friction coefficients, Hassani *et al.* (1997) found that friction drags the upper plate down with the subducting plate, thereby inhibiting the growth of high topography. These results have been confirmed by Buiter *et al*. (2001) for a friction coefficient of $\mu = 0.1$ in a similar set-up; in another model run with a frictionless plate interface, Buiter *et al*. (2001) observed an upward vertical displacement for a trenchward advancing upper plate. In contrast to Hassani *et al.* (1997) and Buiter *et al*. (2001), Cattin *et al.* (1997) used a model in which the ocean plate subducts with a prescribed velocity and slab curvature beneath an elasto-visco-plastic upper plate, which moves toward the trench at a constant velocity. They concluded that friction coefficients of $\mu \leq 0.2$ are required to create and maintain high topography in the upper plate; only friction coefficients of $\mu > 0.2$ tend to drag the upper plate down. The contrary predictions of the different models with respect to interplate coupling, upper plate motion and the development of topography are not easily resolved, since Cattin *et al.* (1997) incorporate a trenchward moving overriding plate but do not account for slab pull, whereas the models of Hassani *et al.* (1997) and Buiter *et al.* (2001) consider slab pull but in a setting with a moving oceanic and fixed upper plate. The differences in the set-ups and results point, however, to the critical role that the delicate interaction between slab pull, interplate coupling, and motion of the upper plate might play for the deformation and the topographic evolution of the overriding plate.

Our study aims to evaluate the role of two parameters, trenchward upper plate motion and interplate coupling, for the growth of topography in the upper plate. We use finite-element models that include an oceanic plate which is driven by slab pull, and is in contact with a continental plate along a frictional plate interface. Following Cattin *et al.* (1997), Hassani *et al.* (1997), and Buiter *et al.* (2001), we represent the sub-lithospheric mantle by applying a basal boundary condition because this allows to study the interaction of the oceanic and continental lithospheres in a numerically feasible way. Two sets of models, in which the upper plate is fixed or moves toward the trench, will be presented. The models are not intended to represent any specific subduction zone but to shed light on the relative importance of the two parameters, upper plate motion and interplate coupling.

## Model set-up

The model consists of a 4000 km-long oceanic plate with a thickness of 80 km and a 2000 km-long continental lithosphere, which is divided into a 30 km-thick crust and a 70 km-thick lithospheric mantle (Fig. 1). Both the oceanic and the continental lithospheres have an elasto-visco-plastic rheology, with a depth-independent Von-Mises yield stress and a temperature-independent linear viscosity. The values of the material properties (*cf*. Turcotte & Schubert 2002; $\rho$ density, E Young's modulus, $\nu$ Poisson's ratio, $\sigma_y$ Von-Mises yield stress, $\eta$ viscosity) are given in Figure 1. At the bottom of the model linear spring and dashpot elements, which mimic the behaviour of an asthenosphere with a density of $\rho = 3200\ \mathrm{kg/m^3}$ and a viscosity of $\eta = 10^{20}$ Pa s, are applied to account for isostatic effects. In addition, a lithostatic pressure equivalent to the overburden is applied to the bottom of the two plates (oceanic plate: 2.6 GPa, continental plate: 3 GPa). The representation of the sub-lithospheric mantle by boundary conditions means that corner flow in the mantle wedge is neglected.

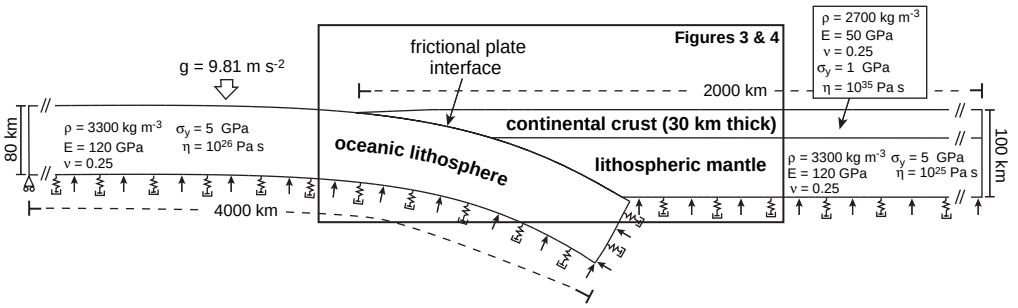


**Fig. 1.** Model set-up with separate oceanic and continental lithospheres that are in contact along the plate interface. Slip on the plate interface is controlled by a Coulomb criterion. The left end of the oceanic lithosphere is free to move in the horizontal direction and fixed in the vertical direction; the right end of the continental plate may not move in the vertical direction and is either fixed (Figs 2a, 3, 5a and 6a) or moves trenchward (Figs 2b, 4, 5b and 6b). Bending stresses in the oceanic plate are calculated separately and imported as pre-stress field (*cf.* Hibbitt *et al.* 2002). In order to include isostatic effects, lithostatic pressure as well as linear spring and dashpot elements that mimic the asthenosphere are applied at the bottom of both plates. See text for explanation of the material properties.

The plate interface is modelled as the contact zone between the two separate meshes of the oceanic plate and the continental plate. Relative tangential motion of the contacting element surfaces is governed by a Coulomb failure criterion with a critical shear stress ($\tau_{\max}$) and a coefficient of friction ($\mu$) (*cf.* ABAQUS, 2002). In the models presented below, the coefficient of friction is increased stepwise from $\mu = 0$ to $\mu = 0.3$. A higher value of the friction coefficient is unrealistic for subduction systems, as indicated by heatflow data and palaeo-geothermal gradients of high-pressure/low-temperature metamorphic rocks (Molnar & England 1990; Kao & Chen 1991; Tichelaar & Ruff 1993).

The calculations have been performed with the ABAQUS/Standard software (ABAQUS, 2002), which uses a Lagrangian formulation and solves the following equation

$$\vec{\nabla}\bar{\bar{\tau}} + \rho\vec{g} = 0$$

where $\bar{\bar{\tau}}$ is the stress tensor, $\rho$ density, and $\vec{g}$ gravitational acceleration. The elements have an average size of $10 \times 10$ km and $5 \times 5$ km for the oceanic and continental plate, respectively; no remeshing is applied. In a first step, the bending stresses in the oceanic plate, which is downflexed owing to a vertical force of $8 \times 10^{13}$ N/m applied to its right edge, are calculated in the absence of the overriding plate (*cf.* Buiter *et al.* 2001; Funiciello *et al.* 2003). In the second step, the continental plate is added and contact is established along the plate interface (this stage of the model is shown in Fig. 1); the system is then allowed to reach isostatic equilibrium again. This procedure avoids the explicit implementation of subduction initiation and allows starting the experiments at a stage at which a slab has already formed. In the third step, the oceanic plate subducts, driven solely by slab pull, which is generated by its own weight and the force applied during the initial phase. No velocity or density anomalies or any additional forces are prescribed on either end of the subducting plate, which is free to move in the horizontal direction. The only boundary condition applied is that the far left edge of the oceanic plate is fixed in the vertical direction. In other words, the subduction velocity of the oceanic plate as well as the curvature of the slab may evolve freely during the main phase of the experiments. The subduction velocity in all models is of the order of a few centimeters per year. The right end of the continental plate is held fixed in the vertical direction. In the first model set presented below, the right edge of the upper plate is fixed in the horizontal direction as well (Figs 2a, 3, 5a and 6a). In the second model set, the boundary condition is such that the upper plate moves toward the trench owing to a displacement of 100 km prescribed at its right edge (Figs 2b, 4, 5b and 6b).

## Results

### *Models with right end of the continental plate fixed*

Figure 3 shows the finite vertical displacement fields for the first set of models, in which the right end of the upper plate is not allowed to move in the horizontal direction. All experiments are run until 200 km of relative slip are reached

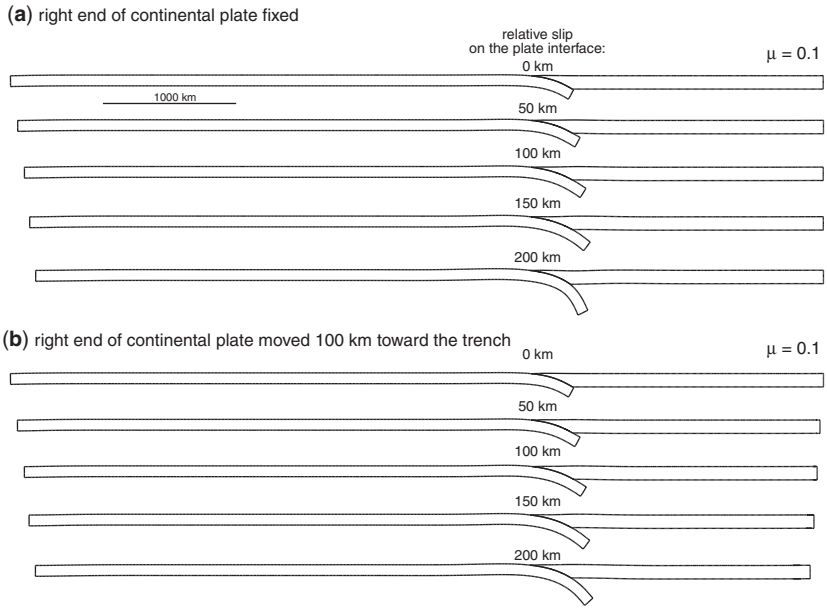


**Fig. 2.** Different stages of the experiments with a friction coefficient of $\mu = 0.1$ (**a**) without and (**b**) with trenchward motion of the upper plate.

on the plate interface; the slip is distributed uniformly on the plate interface. In order to illustrate the development of the entire model, different stages of the experiments performed with $\mu = 0.1$ are shown in Figure 2. For the frictionless case and for a coefficient of friction of $\mu = 0.05$, a broad zone of upward vertical motion develops landward of the intersection between the base of the continental lithosphere and the top of the subducting plate (region C in Fig. 3a, b). For coefficients of friction of $\mu \geq 0.1$, this zone strongly subsides by up to 9 km (regions C in Fig. 3c–e). In contrast, the frontal part of the overriding plate, within a distance of 30–40 km from the trench, is uplifted by *c*. 2 km regardless of the friction coefficient applied (regions A in Fig. 3). Between the uplifted and strongly subsiding regions A and C the upper plate experiences a moderate amount of subsidence of 1–2 km in all models (regions B).

The strong influence of the friction coefficient on the evolution of the models is also revealed in a comparison of their initial and final topographic profiles (Fig. 5a). For $\mu \leq 0.05$, a broad zone, in which the topography is higher than at the initial stage, has developed, whereas in the case of $\mu \geq 0.1$ the upper plate subsides over a wide region, with the width increasing with higher friction coefficients. Note that in all experiments, including the ones with upper plate motion (presented below), the topography evolves continuously from the initial to the final stage.

With respect to the stress field, the subsiding part of the upper plate is associated with a region of curved trajectories of the principal stresses $\sigma_1$ and $\sigma_3$ (shown in the upper panel of Fig. 6a for the model with $\mu = 0.1$). The maximum principal stress is vertical near the base of the lithosphere and perpendicular to the plate interface in its lower part. In the lower left corner of the upper plate, the minimum principal stress attains negative values (lower panel of Fig. 6a). This pattern of the principal stresses indicates that the lower left part of the upper plate is dragged down by the subducting plate. At the surface of the subsiding segment, the maximum principal stress has a horizontal orientation and is higher than in neighbouring regions, which is an expression of the upper plate's flexure resulting from the downward drag induced by the oceanic plate.

### *Models with a trenchward-moving continental plate*

In the second set of experiments, the upper plate moves trenchward by 100 km. The finite vertical displacement fields after 200 km of slip are

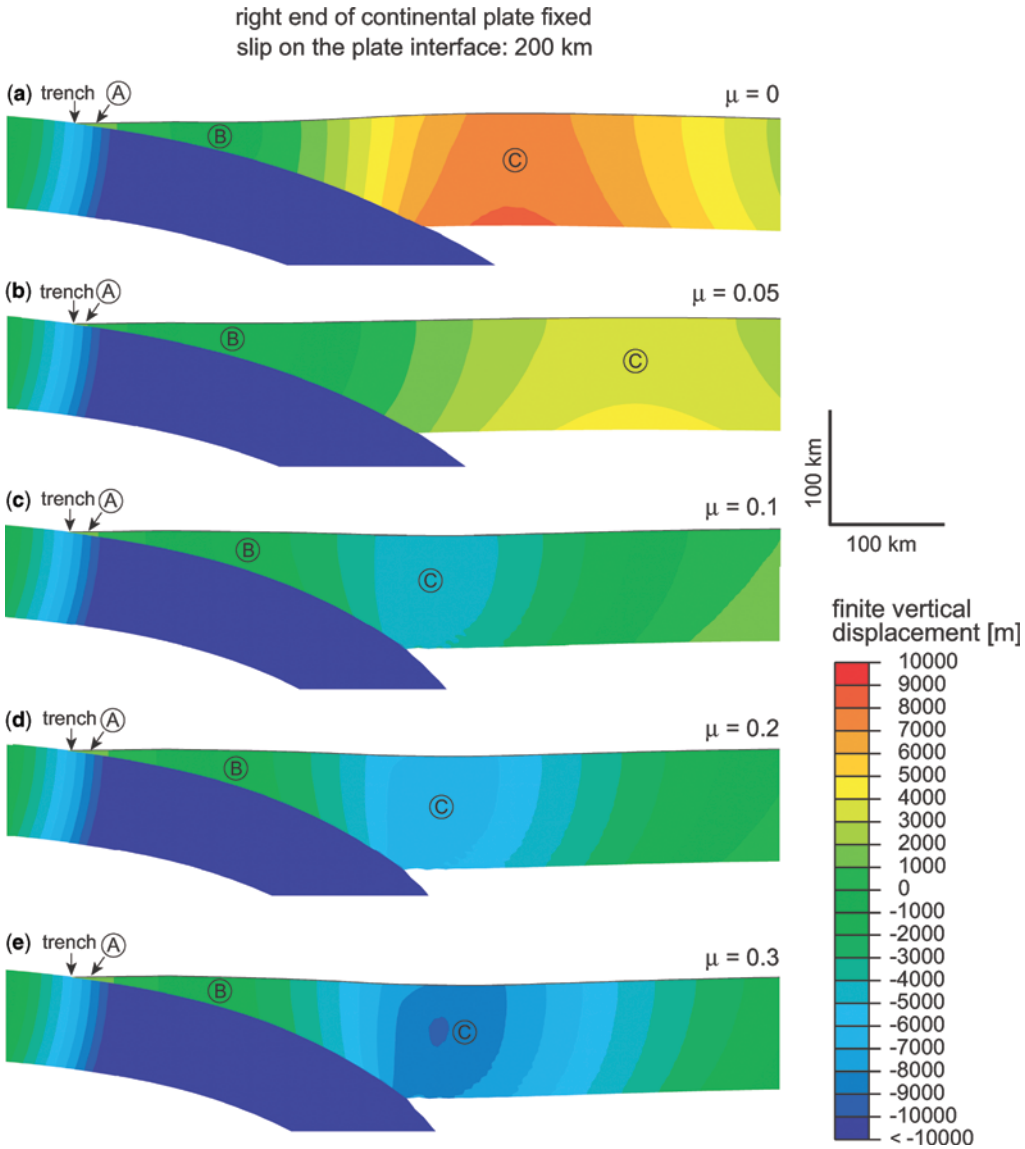


**Fig. 3.** Finite vertical displacement fields after 200 km of slip on the plate interface for the models with the right end of the continental plate fixed in the horizontal direction. Circles at the bottom of the model mark the spring and dashpot elements. Note that friction coefficients of $\mu \geq 0.1$ lead to strong subsidence of the upper plate (regions C) and inhibit the formation of a mountain belt. The frontal part of the upper plate (A) is uplifted; the adjacent part marked by B experiences moderate subsidence by 1–2 km.

depicted in Figure 4. For all coefficients of friction, the overriding plate experiences uplift, however, the uplift pattern differs for low and high friction values. In the presence of a frictionless plate interface, the distribution of uplift is similar to the one observed in the first model set except that the amount of uplift (Fig. 4a) and the final topography (Fig. 5b) is considerably higher. A maximum of ca. 9 km of uplift is reached slightly landward of the intersection of the base of the continental lithosphere and the top of the subducting oceanic plate (region C in Fig. 4a). For $\mu = 0.05$ and $\mu = 0.1$, the zone of highest uplift broadens and lower maximum

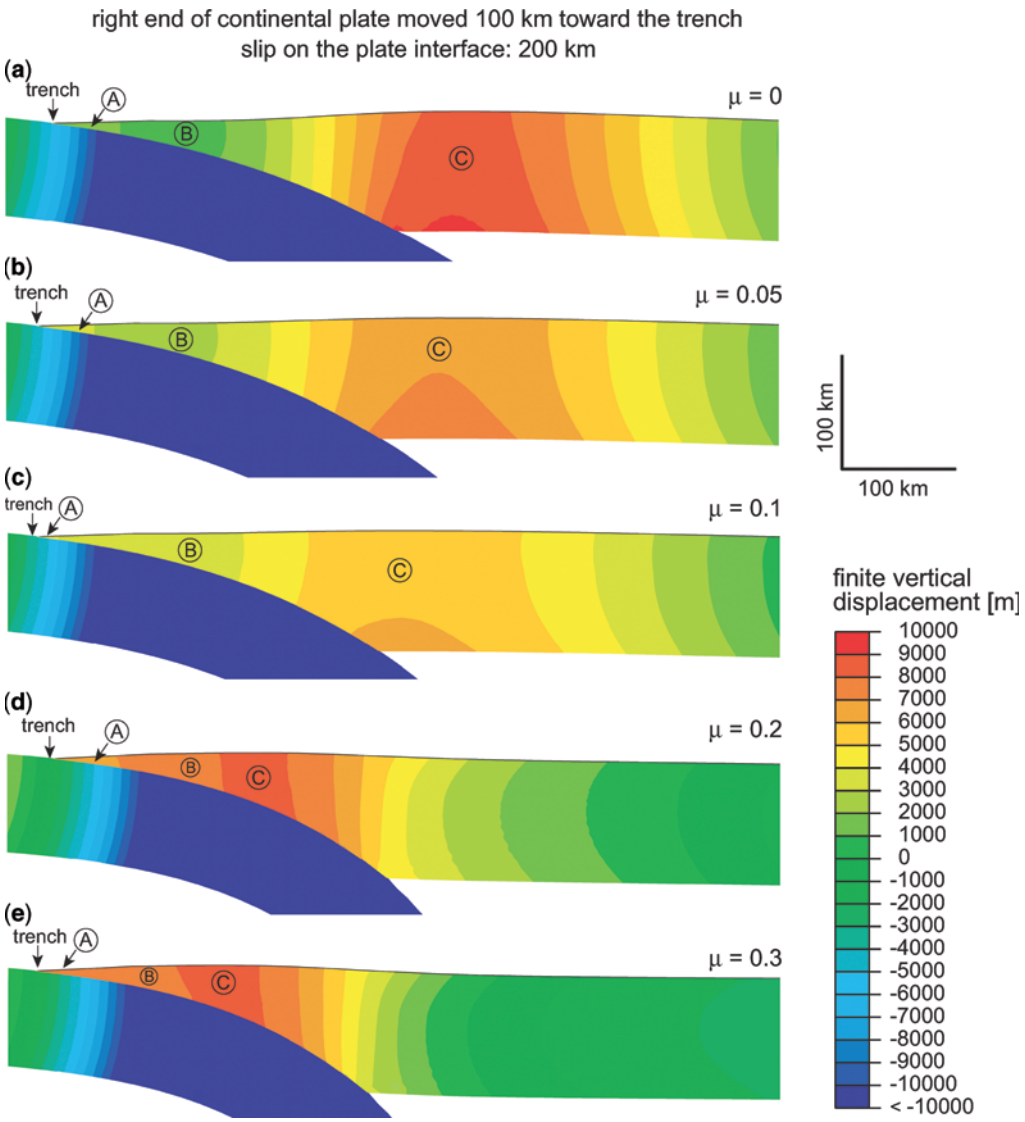


**Fig. 4.** Finite vertical displacement fields after 200 km of slip on the plate interface for the models with the continental plate advancing 100 km toward the trench. Note that for all coefficients of friction, high topography develops in the upper plate, regardless of the coefficient of friction (regions C). In the models with $\mu \leq 0.1$, the frontal part of the upper plate (A) experiences higher uplift than the adjacent region (B). For friction coefficients of $\mu > 0.1$, uplift in the overriding plate localizes above the plate interface (C in d, e).

values of 5–7 km are observed (regions C in Fig. 4b, c). In the three models with $\mu \leq 0.1$, the frontal part of the upper plate (A) is more strongly uplifted than the adjacent region B. The difference between the maximum and minimum upward displacement observed in regions C and B, decreases from 8 km ($\mu = 0$) to 2 km ($\mu = 0.1$) (Fig. 4a, c). For friction coefficients of $\mu > 0.1$, the uplift pattern changes dramatically: the zone of maximum uplift narrows and shifts toward the trench to a position above the centre of the plate interface, where a maximum vertical displacement of 8–9 km is reached (region C in Fig. 4d, e). The trenchward shift of the region with maximum vertical displacement is associated with a shift

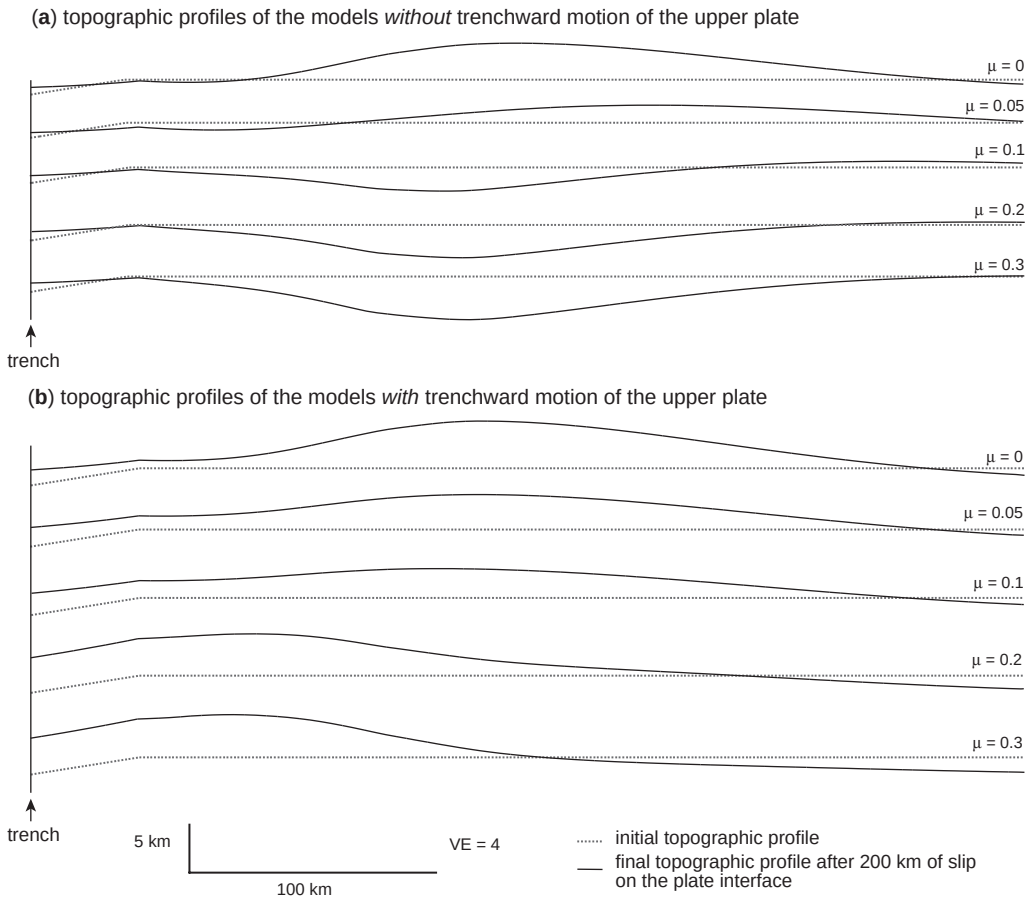


**Fig. 5.** Topographic profiles of the two model sets (**a**) without and (**b**) with trenchward motion of the upper plate. The dotted grey line marks the initial topography (Fig. 1), while the black line indicates the final topographic profile after 200 km of slip on the plate interface.

of the highest topography toward the trench (Fig. 5b). In the models with $\mu \geq 0.1$, the amount of uplift increases continuously from the trench to the region of maximum uplift (C), i.e., region B experiences stronger uplift than the frontal part of the continental plate (A).

The stress field obtained for the models with upper plate motion differs considerably from the one observed for a stationary upper plate (Fig. 6b). The orientation of the principal stresses indicates that the continental plate is under horizontal compression throughout, with the highest values of the maximum principal stress occurring at the lower left corner of the upper plate. With increasing friction, this region of high compressive stresses becomes larger (not shown in Fig. 6).

## Discussion and conclusions

The results of our experiments reveal the crucial role of the upper plate's behaviour for topographic evolution at convergent margins. If the overriding plate remains stationary, the pull of the subducting plate tends to drag it down; this effect is amplified with increasing interplate coupling (Figs 3c–e and 6a). This observation agrees with the modelling results of Hassani *et al.* (1997) and Buiter *et al.* (2001). High topography in the upper plate develops in two cases: (1) if the upper plate remains fixed and the plate interface is frictionless, which is in accordance with Buiter *et al.* (2001), and (2) for $\mu > 0$, if the upper plate advances trenchward. In the latter case, the motion of the overriding plate

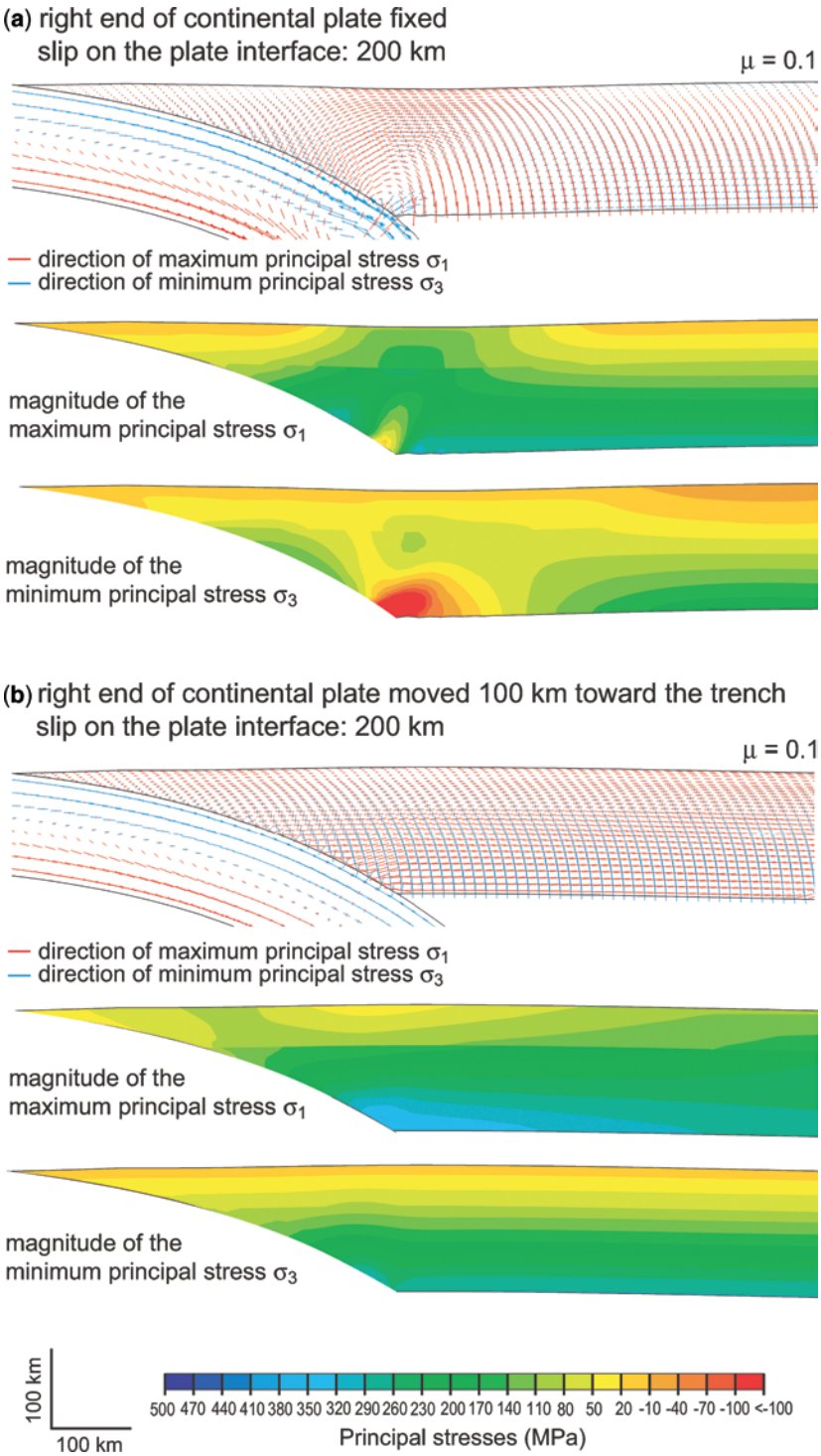


**Fig. 6.** Orientation and magnitude of the maximum and minimum principal stresses in the experiments with a friction coefficient of $\mu = 0.1$; (**a**) without and (**b**) with trenchward motion of the upper plate.

overcomes the downward drag exerted by the subducting plate, which is a combined effect of slab pull and interplate coupling. Thus the growth of high topography is promoted (Fig. 6b). Our model results imply an active role of the continental plate in the mountain-building process and are in general agreement with Cattin *et al.* (1997). These authors report, however, that friction coefficients of $\mu \leq 0.1$ lead to the development of unrealistically high topography, an effect that does not occur in our experiments (Fig. 4a, b). We interpret this significantly different behaviour as a result from the fact that we account for the pull of the slab, which acts against upward displacement of the overriding plate, whereas Cattin *et al.* (1997) did not include slab pull into their models.

With respect to the relationship between the degree of interplate coupling and a high topography, our experiments demonstrate that it may be misleading to infer a high coefficient of friction simply from the presence of high topography, without accounting for the motion of the upper plate. Such an approach was applied, for example, to the Andes (Lamb & Davis 2003). Although the occurrence of strong subduction earthquakes and the absence of a thick sedimentary cover on the oceanic plate in the central segments of the Andean margin support the conclusion of high interplate coupling, the Andes represent an example where the topography and the intracontinental deformation are not solely related to the motion and nature of the oceanic plate. Instead, geological evidence points to a close relationship between intraplate deformation and upper plate motion. For example, the kinematic analyses of fault populations in the central Andes suggest that temporal changes in the contraction directions reflect the *absolute South American* plate motions during the last 20.5 Ma (Marrett & Strecker 2000) rather than the Nazca–South American relative motion (e.g., Hindle *et al.* 2002; Riller & Oncken 2003), which is dominated by the absolute motion of the Nazca Plate. Faults in the Eastern Cordillera of northwestern Argentina and southern Bolivia indicate WNW–ESE shortening from the Miocene until the Pliocene (Marrett *et al.* 1994; Müller *et al.* 2002). During this time span, from 20.5 Ma to 3.2 Ma, South America moved west–northwestward (Pardo-Casas & Molnar 1987). Since 2–3 Ma, ENE–WSW shortening dominates on the faults (Marrett & Strecker 2000). At 3.2 Ma, South America changed to the west–southwestward direction still maintained today (Pardo-Casas & Molnar 1987; DeMets *et al.* 1990; Norabuena *et al.* 1998). This strongly suggests a causative relation between intraplate contraction and the westward advance of the South American plate, which has been faster than the rollback of the Nazca plate (Marrett & Strecker 2000). South America's absolute motion is primarily caused by the push of the South Atlantic ridge, which leads to a westward motion of both the mid-ocean ridge and South America relative to an approximately stable African Plate (Meijer & Wortel 1992; DeMets *et al.* 1990).

In conclusion, our model results indicate that the motion of the overriding plate plays a key role in the formation of mountain belts at convergent margins. Depending on the behaviour of the overriding plate, friction along the plate interface either leads to subsidence or amplifies crustal shortening and the growth of topography in the upper plate.

We wish to thank the editors, S. Buiter and G. Schreurs, who also co-organized the extremely stimulating GEOMOD 2004 conference in Emmetten at the Lake Lucerne, Switzerland, for their efforts. The thoughtful comments by S. Buiter and by the reviewers M. Gerbault, R. de Franco, and R. Govers improved the manuscript. A. H. thanks R. Hetzel for critical comments on earlier versions of the manuscript. Funding for the project was provided by the Swiss National Science Foundation (grant no. 2000-067952).

## References

ABAQUS/Standard User's Manual, 2002. Version 6.3, Hibbitt, Karlson and Sorenson, Inc., Pawtucket, RI, USA.

BEVIS, M., KENDRICK, E., SMALLEY, R., BROOKS, B., ALLMENDINGER, R. & ISACKS, B. 2001. On the strength of interplate coupling and the rate of backarc convergence in the central Andes: an analysis of the interseismic velocity field. *Geochemistry, Geophysics, Geosystems ($G^3$)*, **2**, 2001GC000198.

BILLEN, M. I. & GURNIS, M. 2001. A low viscosity wedge in subduction zones. *Earth and Planetary Science Letters*, **193**, 227–236.

BOTT, M. H. P., WAGHORN, G. D. & WHITTAKER, A. 1989. Plate boundary forces at subduction zones and trench-arc compression. *Tectonophysics*, **170**, 1–15.

BUITER, S. J. H., GOVERS, R. & WORTEL, M. J. R. 2001. A modelling study of vertical surface displacements at convergent plate margins. *Geophysical Journal International*, **147**, 415–427.

CATTIN, R., LYON-CAEN, H. & CHERY, J. 1997. Quantification of interplate coupling in subduction zones and forearc topography. *Geophysical Research Letters*, **24**, 13, 1563–1566.

CHASE, C. G. 1978. Extension behind islands arcs and motions relative to hot spots. *Journal of Geophysical Research*, **83**, 5385–5387.

CONRAD, C. P., BILEK, S. & LITHGOW-BERTELLONI, C. 2004. Great earthquakes and slab pull: interaction between seismic coupling and plate-slab coupling. *Earth and Planetary Science Letters*, **218**, 109–122.

DEMETS, C., GORDON, R. G., ARGUS, D. F. & STEIN, S. 1990. Current plate motions. *Geophysical Journal International*, **101**, 425–478.

DEWEY, J. F. & LAMB, S. H. 1992. Active tectonics of the Andes. *Tectonophysics*, **205**, 1–3, 79–95.

DMOWSKA, R., ZHENG, G. & RICE, J. R. 1996. Seismicity and deformation at convergent margins due to heterogeneous coupling. *Journal of Geophysical Research*, **101**, B2, 3015–3029.

ENGLAND, P. & WORTEL, R. 1980. Some consequences of the subduction of young slabs. *Earth and Planetary Science Letters*, **47**, 403–415.

FORSYTH, D. & UYEDA, S. 1975. On the relative importance of the driving forces of plate motion. *Geophysical Journal of the Royal Astronomical Society*, **43**, 163–200.

FUNICIELLO, F., MORRA, G., REGENAUER-LIEB, K. & GIARDINI, D. 2003. Dynamics of retreating slabs: 1. Insights from two-dimensional numerical experiments. *Journal of Geophysical Research*, **108**, B4, 2206, DOI 10.1029/2001JB000898.

GEPHART, J. 1994. Topography and subduction geometry in the central Andes: clues to the mechanics of a noncollisional orogen. *Journal of Geophysical Research*, **99**, 12279–12288.

HAMILTON, W. B. 1995. Subduction systems and magmatism. *In*: SMELLIE, J. L. (ed.) *Volcanism Associated with Extension at Consuming Plate Margins*, Geological Society Special Publications, **81**, 3–28.

HAMILTON, W. B. 2003. An alternative Earth. *GSA Today*, **13**, 11, 4–12, DOI 10.1130/1052-5173.

HASSANI, R., JONGMANS, D. & CHÉRY, J. 1997. Study of plate deformation and stress in subduction processes using two-dimensional numerical models. *Journal of Geophysical Research*, **108**, 17951–17965.

HINDLE, D., KLEY, J., KLOSKO, E., STEIN, S., DIXON, T. & NORABUENA, E. 2002. Consistency of geologic and geodetic displacements during Andean orogenesis. *Geophysical Research Letters*, **29**, 8, 2001GL013757.

HUANG, S. S., SACKS, I. S. & SNOKE, J. A. 1998. Compressional deformation of island-arc lithosphere in northeastern Japan resulting from long-term subduction-related tectonic forces: finite-element modeling. *Tectonophysics*, **287**, 1–4, 43–58.

HEURET, A. & LALLEMAND, S. 2005. Plate motions, slab dynamics and back-arc deformation. *Physics of the Earth and Planetary Interiors*, **149**, 31–51.

HUSSON, L. & RICARD, Y. 2004. Stress balance above subduction: application to the Andes. *Earth and Planetary Science Letters*, **222**, 1037–1050.

JARRARD, R. D. 1986. Relations among subduction parameters. *Reviews of Geophysics*, **24**, 217–284.

JORDAN, T. E., ISACKS, B. L., ALLMENDINGER, R. W., BREWER, J. A., RAMOS, V. A. & ANDO, C. J. 1983. Andean tectonics related to geometry of subducted Nazca Plate. *Geological Society of America Bulletin*, **94**, 3, 341–361.

KAO, H. & CHEN, W. P. 1991. Earthquakes along the Ryukyu-Kyushu arc: strain segmentation, lateral compression, and thermomechanical state of the plate interface. *Journal of Geophysical Research*, **96**, 21443–21485.

LAMB, S. & DAVIS, P. 2003. Cenozoic climate change as a possible cause for the rise of the Andes. *Nature*, **425**, 792–797.

MARRETT, R. & STRECKER, M. R. 2000. Response of intracontinental deformation in the central Andes to late Cenozoic reorganization of the South American Plate motions. *Tectonics*, **19**, 3, 452–467.

MARRETT, R., ALLMENDINGER, R. W., ALONSO, R. N. & DRAKE, R. E. 1994. Late Cenozoic tectonic evolution of the Puna Plateau and adjacent foreland, northwestern Argentine Andes. *Journal of South American Earth Sciences*, **7**, 179–207.

MEIJER, P. T. & WORTEL, M. J. R. 1992. The dynamics of motion of the South American Plate. *Journal of Geophysical Research*, **97**, 11915–11931.

MOLNAR, P. & ATWATER, T. 1978. Interarc spreading and cordilleran tectonics as alternates related to the age of subducted oceanic lithosphere. *Earth and Planetary Science Letters*, **41**, 330–340.

MOLNAR, P. & ENGLAND, P. 1990. Temperatures, heat flux, and frictional stress near major thrust faults. *Journal of Geophysical Research*, **95**, 4833–4856.

MÜLLER, J. P., KLEY, J. & JACOBSHAGEN, V. 2002. Structure and Cenozoic kinematics of the Eastern Cordillera, southern Bolivia (21°S). *Tectonics*, **21**, 5, 1037, DOI 10.1029/2001TC001340.

NICOL, A. & BEAVAN, J. 2003. Shortening of an overriding plate and its implications for slip on a subduction thrust, central Hikurangi Margin, New Zealand. *Tectonics*, **22**, 6, 1070.

NORABUENA, E., LEFFLER-GRIFFIN, L. *ET AL.* 1998. Space geodetic observations of Nazca-South American convergence across the central Andes. *Science*, **279**, 358–362.

PARDO-CASAS, F. & MOLNAR, P. 1987. Relative motion of the Nazca (Farallon) and South American Plates since Late Cretaceous time. *Tectonics*, **6**, 233–248.

RILLER, U. & ONCKEN, O. 2003. Growth of the Central Andean Plateau by tectonic segmentation is controlled by the gradient in crustal shortening. *Journal of Geology*, **111**, 367–384.

ROYDEN, L. H. 1993. The tectonic expression of slab pull at continental convergent plate boundaries. *Tectonics*, **12**, 303–325.

RUFF, L. & KANAMORI, H. 1980. Seismicity and the subduction process. *Physics of the Earth and Planetary Interiors*, **23**, 240–252.

SCHOLZ, C. H. & CAMPOS, J. 1995. On the mechanism of seismic decoupling and backarc spreading at subduction zones. *Journal of Geophysical Research*, **100**, B11, 22103–22115.

SHEMENDA, A. 1993. Subduction of the lithosphere and backarc dynamics: insights from physical modeling. *Journal of Geophysical Research*, **98**, B9, 16167–16185.

STERN, R. J. 2002. Subduction zones. *Reviews of Geophysics*, **40**, 4, 1012, DOI 10.1029/2001RG000108.

TICHELAAR, B. W. & RUFF, J. L. 1993. Depth of seismic coupling along subduction zones. *Journal of Geophysical Research*, **98**, 2017–3027.

TURCOTTE, D. L. & SCHUBERT, G. 2002. *Geodynamics*, Cambridge University Press, 2nd edition.

UYEDA, S. & KANAMORI, H. 1979. Backarc opening and the mode of subduction. *Journal of Geophysical Research*, **84**, 1049–1061.

WANG, K. L. & HE, J. H. 1999. Mechanics of low-stress forearcs: Nankai and Cascadia. *Journal of Geophysical Research*, **104**, B7, 15191–15205.

WDOWINSKI, S., O'CONNELL, R. J. & ENGLAND, P. 1989. A continuum model of continental deformation above subduction zones: application to the Andes and the Aegean. *Journal of Geophysical Research*, **94**, 10331– 10346.

WILLETT, S. D., BEAUMONT, C. & FULLSACK, P. 1993. Mechanical model for the tectonics of doubly vergent compressional orogens. *Geology*, **21**, 371–374.

YANEZ, G. & CEMBRANO, J. 2004. Role of viscous plate coupling in the late Tertiary Andean tectonics. *Journal of Geophysical Research*, **109**, B02407, 15191–15205, DOI 10.1029/2003JB002494.